

Mass balance, flow, and subglacial processes of a modelled Younger Dryas ice cap in Scotland

Nicholas R. GOLLEDGE,^{1,2} Alun L. HUBBARD,³ David E. SUGDEN,²

¹*British Geological Survey, Murchison House, West Mains Road, Edinburgh, EH9 3LA**

Email: n.golledge@bgs.ac.uk

²*Institute of Geography, University of Edinburgh, Drummond Street, Edinburgh, EH8 9XP*

³*Institute of Geography & Earth Sciences, The University of Wales, Aberystwyth, Ceredigion, SY23 3DB*

ABSTRACT. We use an empirically validated high-resolution three-dimensional ice sheet model to investigate the mass balance regime, flow mechanisms, and subglacial characteristics of a simulated Younger Dryas stadial ice cap in Scotland, and compare the resulting model forecasts with geological evidence. Input data for the model are basal topography, a temperature forcing derived from GRIP $\delta^{18}\text{O}$ fluctuations, and a precipitation distribution interpolated from modern data. The model employs a Positive Degree Day scheme to calculate net mass balance within a domain of 112500 km², which under the imposed climate gives rise to an elongate ice cap along the axis of the western Scottish Highlands. At its maximum, the ice cap is dynamically and thermally zoned, reflecting topographic and climatic controls respectively. In order to link these palaeoglaciological conditions to geological interpretations, we calculate the relative balance between sliding and creep within the simulated ice cap; forecast areas of the ice cap with the greatest capacity for basal erosion; and predict the likely pattern of subglacial drainage. We conclude that ice flow in central areas of the ice cap is a largely due to internal deformation, and is associated with geological evidence of landscape preservation. Conversely, the distribution of streamlined landforms is linked to faster-flowing ice whose velocity is predominantly the result of basal sliding. The geometry of the main ice mass focusses subglacial erosion in the mid-sections of topographic troughs, and produces glaciohydraulic gradients that favour subglacial drainage through low-order arterial routes.

INTRODUCTION

The Younger Dryas cold episode (12.7–11.5 ka BP, Alley, 2000) was marked in the Northern Hemisphere by the expansion of the Laurentide and Fennoscandian ice sheets, and by a partial regrowth of the British Ice Sheet (Sutherland, 1984; Mangerud, 1991; MacAyeal, 1993). Understanding the evolution of these former ice sheets helps appreciation of contemporary ice masses and their likely behavioural response to future climate change scenarios. Attempts to reconstruct former glaciers commonly focus on the identification and interpretation of empirical (geological) data within a relatively small area, and permit only local-scale interpretations of glaciers either at their maximum extent or during their retreat. In Scotland this geological approach is complicated by the variable overprinting, reworking or complete removal of landforms relating to the Main Late Devensian ice sheet by those of the much smaller, later, Younger Dryas ice cap (e.g. Golledge, 2006). Consequently, geological studies are commonly hampered by their limited ability to accurately constrain marginal contemporaneity, and so struggle to evince details of glacier mass balance or flow characteristics. Numerical modelling of glaciers and ice sheets allows insight into these areas, by simulating ice masses and their governing climates and most importantly, by enabling the interpretation of glacier evolution through a glacial episode (e.g. Siegert and Dowdeswell, 2004). This temporal element is of great importance when trying to identify and differentiate dynamically and climatically forced

margin oscillations, and promotes a more complete understanding of the surviving geological record.

Despite the clear benefits of a combined geological and modelling analysis, previous attempts at numerical simulations of Younger Dryas glaciers in Scotland are relatively uncommon (e.g. Payne and Sugden, 1990; Hubbard, 1999), and rarely incorporate explicit field data. In order to address such shortcomings, Golledge and others (2008) presented an empirically validated ice sheet model for Scotland for the Lateglacial period (15–11 ka BP). In this article we aim to:

1. explore the mass balance regime of the modelled ice cap during its evolution
2. calculate the balance between flow by internal deformation and flow resulting from basal sliding, and its spatial variability, during the height of the Stadial
3. calculate the likely pattern of erosion potential of the modelled ice cap and identify areas where greatest basal erosion might occur
4. predict the spatial organisation of subglacial hydrology beneath the ice cap
5. compare these model results with empirical evidence in western Scotland in order to more confidently link geological features with former glaciological conditions

*Address for correspondence

THE MODEL

The three-dimensional finite-difference ice sheet model uses algorithms developed and validated by Hubbard (1999) and Hubbard and others (2005, 2006). For the experiments presented here, this thermomechanical model uses a domain of 300 x 375 km, with basal topography at 500 m horizontal resolution derived from Intermap's 1.2 m vertical resolution NextMAP terrestrial elevation data and British Geological Survey 10 m vertical resolution marine bathymetric data.

Mean annual air temperature and mean annual precipitation are calculated from the United Kingdom Climatic Impacts Programme (UKCIP) dataset (Perry and Hollis, 2005), which provides 5 km resolution data for the entire United Kingdom (UK), interpolated from a national network of 3500 weather stations. Whilst recognising the benefits of integrating ice sheet models with atmospheric general circulation models (AGCM), we consider this high-resolution, locally derived, UKCIP dataset to be more suitable as input data than climatic parameters derived from the relatively coarse AGCMs, which are more suitable for use in hemispheric-scale ice sheet modelling (e.g. Siegert and Dowdeswell, 2004). Use of linear interpolations of climate trends between individual 'snapshots' has undoubtedly facilitated greater integration of AGCMs with ice sheet models, but in some cases such generalisation completely removes short-lived climatic events such as the Younger Dryas (e.g. interpolation between timeslices at 15 ka and 9 ka BP of Charbit and others, 2002). Use of local-scale data is thus preferable for these experiments, but introduces the possibility that quite different model scenarios may result if other climate forcings are used.

An elevation-related Positive Degree Day (PDD) scheme drives mass balance by calculating annual accumulation and melt through integration of the snow – rainfall ratio, the amount of refreezing, and the net altitude-related snow balance, following Laumann and Reeh (1993). Input temperatures are computed using a sinusoidal annual temperature variation fluctuating within a range, and from a mean annual temperature, derived from the UKCIP dataset. Precipitation is distributed evenly through the year. Use of a PDD scheme such as this, in preference to a full energy-balance algorithm, is the only pragmatic option where palaeo-data for the latter are lacking (e.g. long- and short-wave radiation balance, wind flux, albedo etc). We further modify accumulation and ablation patterns by imposing eastward and northward precipitation reductions away from the main ice mass, of 80% and 60% respectively (Golledge and others, 2008). Variations in GRIP 20-year resolution $\delta^{18}\text{O}$ data (Johnsen and others, 2001) are used to define the pattern of temperature fluctuation in the model domain, which is scaled to Scottish palaeotemperatures by analogy with modern isotopic values in Greenland (Clapperton, 1997) (Figure 1). Use of the GRIP temperature pattern as a suitable proxy from Scotland is supported by the close similarity between temperature trends observed in its isotopic variations and those inferred from palaeoecological proxies in the UK (Atkinson and others, 1987; Kroon and others, 1997; Brooks and Birks, 2000). Furthermore, palaeoglaciological studies in Ireland have established that glacier fluctuations there were broadly consistent with isotopic trends evident in the GRIP record during the Younger Dryas, despite being out-of-phase prior to c. 17

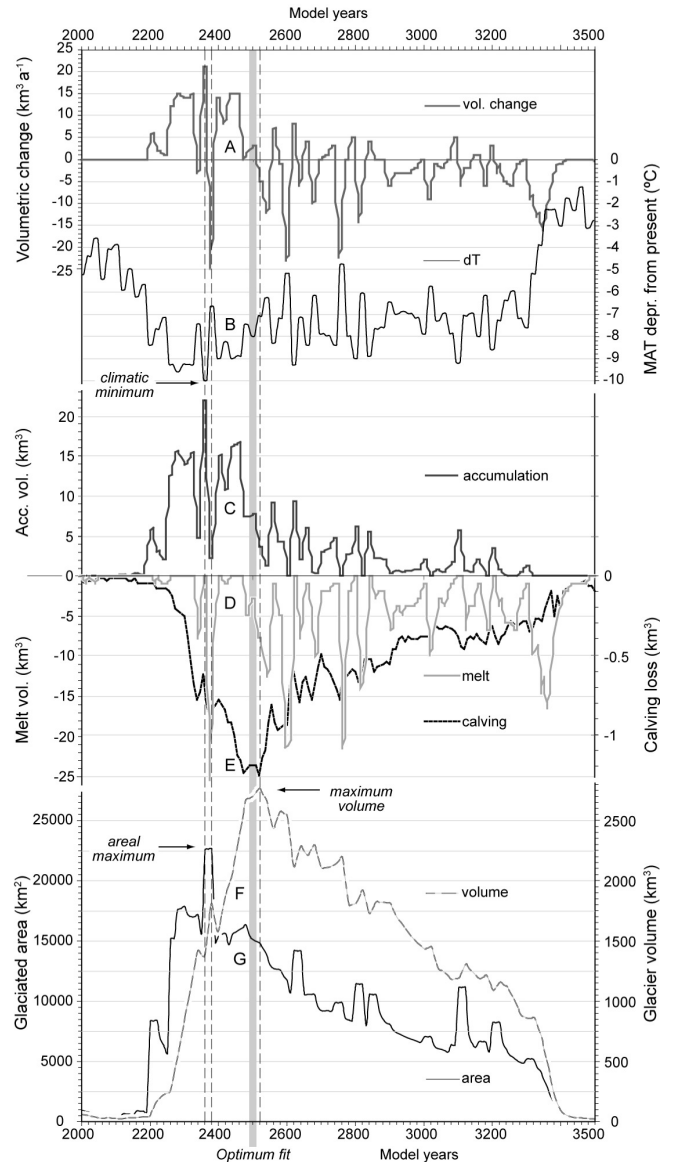


Fig. 1. Mass balance parameter and forcing temperature variability through the Younger Dryas model run, showing A: fluctuations in rate of annual volumetric change, B: the 20-year resolution temperature pattern used to force the model run, C, D, E: accumulation, annual melt, and annual calving volumes, F, G: changes in net volume and areal extent of ice in the domain. Note lag between climatic minimum and maximum ice volume.

ka BP (Knight, 2003). Spatial variability of modelled surface temperatures and precipitation inputs across the domain at the height of the Stadial is shown in Figure 2.

Net mass balance (b) is related to the three-dimensional evolution of the ice cap through time (t) through the equation for the conservation of mass, based on the assumption that ice is incompressible:

$$\frac{\partial H}{\partial t} = b - \nabla \cdot (H\bar{u}) \quad (1)$$

where H is ice thickness, t is time, \bar{u} is the vertically averaged horizontal velocity, and ∇ represents the ice flux between adjacent nodes minus surface mass balance. Ice velocity is composed of internal deformation (Glen, 1955), and Weertman-type sliding when basal temperatures are sufficient to gen-

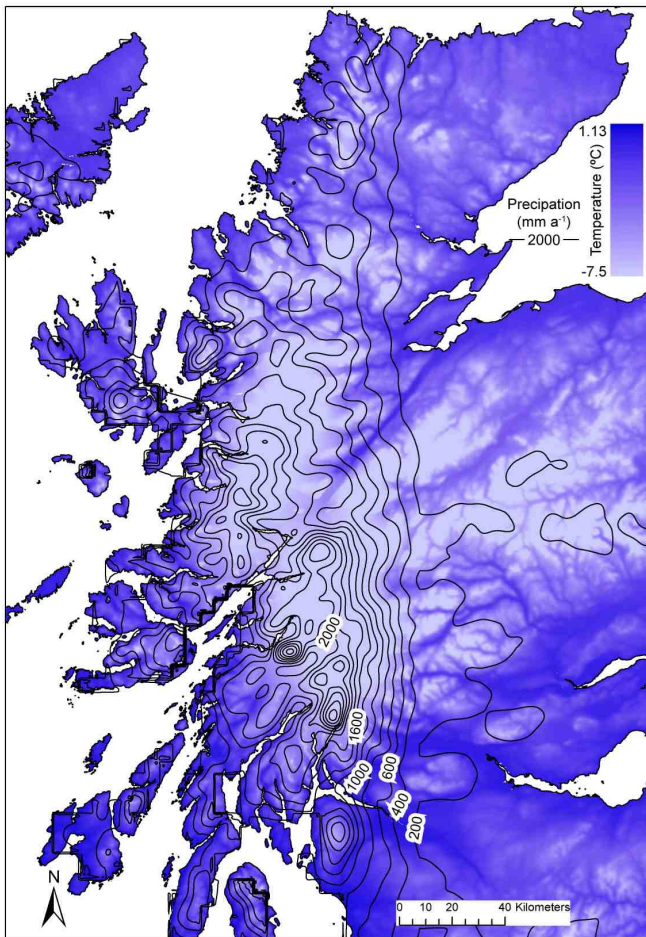


Fig. 2. Modelled surface temperatures across the domain at 2500 model years, and contoured annual precipitation totals. Temperatures incorporate cooling due to altitude; precipitation pattern reflects imposed eastward and northward reductions simulating aridity away from the main ice mass.

erate pressure melting, and is determined through calculation of basal shear stresses corrected by a term for the vertically averaged longitudinal deviatoric stress. The basis and full derivation of this empirically validated ice-stretching algorithm are presented elsewhere (Hubbard, 1999, 2000, 2006), and so are not reiterated here. Many studies have found that water depth exerts the principal control on the rate of calving at water-terminating glacier margins (e.g. Zweck and Huybrechts, 2003). We employ a relatively simple scheme which calculates mass lost due to calving (U_c) as a product of ice thickness, (H), water depth, (W_d), and a calving parameter (A_c) (Brown and others, 1982; van der Veen, 1999) (Equation 2):

$$U_c = A_c H W_d \quad (2)$$

This crude approximation of calving is clearly less preferable than more complex relationships (e.g. Benn and others, 2007a,b) but is computationally less intensive and is a reasonable solution in our domain, where calving losses are close to zero through much of the model run. Sea level is parameterised at +10 m for the duration of the model run, in accordance with empirical sea level reconstructions for this time period from coastal areas of western Scotland (Peacock and others, 1977; Shennan and others, 1999). Although this parameterisation of calving and sea level altitude has allowed

many west coast glacier limits to be faithfully reproduced by the model (Golledge and others, 2008), we acknowledge that using different functions and parameter values may have a significant effect on overall ice cap geometry by locally altering the ablation component of the ice cap's mass balance. Our domain topography does not include the bathymetry of freshwater bodies, which may also introduce local errors in areas where particularly deep lochs occur (e.g. Loch Lomond).

Thermal evolution of the ice sheet through time ($\partial T/\partial t$) is calculated according to the relationship:

$$\frac{\partial T}{\partial t} = \frac{k_{ice}}{\rho_{ice} C_p} \nabla^2 T - \vec{u} \cdot \nabla T + \frac{\Phi}{\rho_{ice} C_p} \quad (3)$$

in which k_{ice} and C_p are the temperature dependent parameters of conductivity and specific heat capacity, \vec{u} is the three-dimensional velocity vector and Φ denotes frictional heat resulting from internal strain (Hubbard, 2006).

The model evolves through a 4000 year run from initially ice-free conditions at 15 ka BP to complete deglaciation by 11 ka BP. A 0.02 year time-step is used in order to most effectively balance model stability against computation time. The spin-up period of 2000 model years (15–13 ka BP) prior to the Younger Dryas episode described here (13–11 ka BP) resulted in intermittent ice growth related to fluctuations in the imposed temperature depression, but almost complete loss of ice from the model domain by 1600 model years. Optimal parameterisation was achieved through a series of sensitivity experiments designed to gauge the relative influence of changes in temperature forcing, precipitation distribution, and the amount of basal sliding, which are described in detail elsewhere (Golledge and others, 2008). The relative closeness of fit of the numerical simulation to empirical reconstructions through the model run is calculated and logged using a grid-comparison algorithm that compares model outputs against empirical reconstructions in five zones (Golledge and others, 2008). This enabled the ‘best-fit’ timeslice to be objectively identified where domain mismatch is at its minimum, which was found to occur between 2400 - 2600 model years. In general, outlying icefields reached their maxima earlier than the outlet glaciers of the main ice cap, which showed greater evidence of lags in the transfer of mass through the glacier system (Golledge and others, 2008). Reduction of annual precipitation totals *during* the Stadial was necessary in order to control ice sheet mass balance and to prevent a ‘run-away’ scenario that produced an implausible glacier configuration. This enhanced aridity of up to 50% at the height of the Younger Dryas (2500 model years), returning to normal conditions towards the end of the stadial, is consistent with inferences from palaeoenvironmental proxies in western Scotland (Benn and others, 1992). That the resulting simulation closely approximates the distribution of ice cover during the Younger Dryas glaciation in Scotland is demonstrated by close agreement of modelled maximal ice margins with geologically reconstructed Younger Dryas ice limits (cf. Sissons, 1979; Ballantyne, 1989, 2002; Clark and others, 2004), and concurrence between spatial variations of modelled ice cap characteristics and interpretations of geological data in the south-east sector of the ice cap (cf. Golledge, 2006, 2007a,b; Golledge and Phillips, 2008).

Table 1. Mass balance parameters through the model run.

Parameter (km ³ a ⁻¹)	Range	Thickness equiv. (m)	YD Max.	Thickness equiv. (m)
Accumulation	0 - 22.1	0 - 1.0	7.7	0.5
Melt	0 - -26.8	0 - -1.2	-3.7	-0.2
Calving loss	0 - -1.2	0 - -0.1	-1.2	-0.1
Net vol. change	21.6 - -24.9	0.9 - -1.1	3.3	0.2

MODEL RESULTS

Mass balance

The scaled GRIP-pattern PDD scheme used to drive the mass balance component of the model couples interpolated horizontal changes in precipitation and temperature across the domain with calculated vertical changes resulting from topography. Figures 1A-G show aspects of climatic and glacier evolution through the Younger Dryas model run; Table 1 describes the variability of mass balance parameters and values at the ‘Optimum fit’ timeslice of 2500 model years. Annual accumulation peaks at approximately +1 ma⁻¹ (Table 1) during the coldest part of the stadial, from around 2370 model years, producing a net annual volumetric increase of 21.6 km³ (Figure 1A). Annual ablation rates achieve a maximum of -1.2 ma⁻¹ (equivalent to a net decrease in volume of 24.9 km³) only a decade later, due to an abrupt (but short-lived) warming oscillation in the GRIP-based temperature curve. Although these extreme values are not subsequently repeated, the lesser peaks evident in Figure 1A nonetheless illustrate the sensitivity of the mass balance model to transient high-magnitude climate oscillations that occur throughout the stadial (Figure 1B). Net accumulation through the Younger Dryas (Figure 1C) integrates losses due to melting (Figure 1D), and calving (Figure 1E). Net accumulation is greatest during the short-lived climatic minimum and decreases subsequently as melting increases (due to the warming climate) and as the ice mass expands to the west coast and calving losses increase. Calving is, however, negligible throughout much of the stadial, exceeding 1 km³a⁻¹ only between 2460 - 2540 model years when ten west coast glaciers are marine-terminating. Figures 1F & G illustrate the integrated consequences of transient mass balance perturbations through the stadial, describing changes in total ice volume and total ice extent respectively. The latter peaks shortly after the lowest temperatures, due to the immediate lowering of the climatic equilibrium line altitude (ELA), whereas ice volume in the domain does not reach its maximum until 2520 model years, 150 years after the thermal nadir. At the ‘Optimum fit’ timeslice of 2500 model years, the Younger Dryas ice cap exhibits relatively low mass-turnover, and a net mean thickening of 0.2 ma⁻¹ (Table 1), comparable with current rates in central-northwest Greenland (Johnsen and others, 1995; Dethloff and others, 2002).

These results highlight considerable high-magnitude short-term variability in the mass balance regime of the ice cap during the Younger Dryas, which initially show a positive bias and lead to rapid ice cap growth at the onset of the stadial. A shift to more generally negative balance after c. 2500 model years (Figure 1A) results in incremental ice cap decay during

Table 2. Parameter ranges, means and variance at optimum fit, 2500 model years.

Parameter	Range	Mean (\bar{x})	Std. Dev. (σ)
Driving stress (kPa)	0 - 164.9	45.6	21.1
Surface slope (%)	0 - 35.9	4.98	4.5
Surface velocity (ma ⁻¹)	0 - 547.6	20.6	36.2
Basal velocity (ma ⁻¹)	0 - 314.9	9.1	18.5
Surface temperature (°C)	1.1 - -7.51	-0.65	1.39
Basal temperature (°C)	0 - -5.91	-0.84	1.26
Total melt (mm/a ⁻¹)	0 - 3.7	0.38	0.4

the remainder of the stadial, culminating in almost complete deglaciation around 3300 - 3500 model years (Figure 1F & G), when net mass balance is overwhelmingly negative (Figure 1A) and results in the loss of c. 1000 km³ ice in 150 years (Figure 1G).

Velocity and flow mechanisms

At the optimum fit timeslice of 2500 model years (12.5 ka BP), surface velocities of modelled glaciers in the domain commonly exceeding 100 ma⁻¹, with some achieving a maximum of nearly 550 ma⁻¹ (Table 2). Figure 3A shows the vertically integrated mean velocity distribution across the ice cap at this time. High velocities in outlet glaciers contrast with much of the interior of the ice cap being relatively static. The maritime icefields on Skye and Mull host zones of relatively fast flow but eastern plateau icefields (Cairngorms, Monadhliath) are largely inactive. Even within the main ice cap, the majority of faster-flowing ice occurs on the west rather than east. This west-east asymmetry is particularly clearly shown in the differences between the Loch Linnhe area glaciers in the west, and those in the east such as the Rannoch glacier (Figure 3B & C).

In order to establish such regional contrasts more easily, we calculate catchment-averaged velocities and mean temperatures across the domain (Figure 4A & B). These summaries integrate surface and basal values at all points within each glacier catchment, and serve to illustrate the dominance of western glaciers in dynamical aspects of the ice cap, in contrast to eastern areas that are colder and flow more slowly. In particular, Figure 4A highlights the importance of Loch Linnhe and Loch Etive as sinks for the largest contiguous area of relatively fast-flowing ice, focussing drainage from mountainous areas both north and south of the Great Glen.

From surface and basal ice velocities (V_s and V_b respectively) it is possible to calculate the proportion of glacier flow that results from basal sliding and from internal deformation (creep) of the ice above the glacier bed. Since surface velocity (V_s) also represents total velocity, which is the sum of basal sliding plus internal deformation, we calculate the velocity due to creep from $V_s - V_b$, making the assumption that any deformation of ice at the glacier bed will probably result in pressure melting and facilitate sliding, thereby reducing the creep component of basal motion to close to zero. Using this approach we can calculate the relative proportion of flow occurring as a result of each mechanism, by defining the relationship:

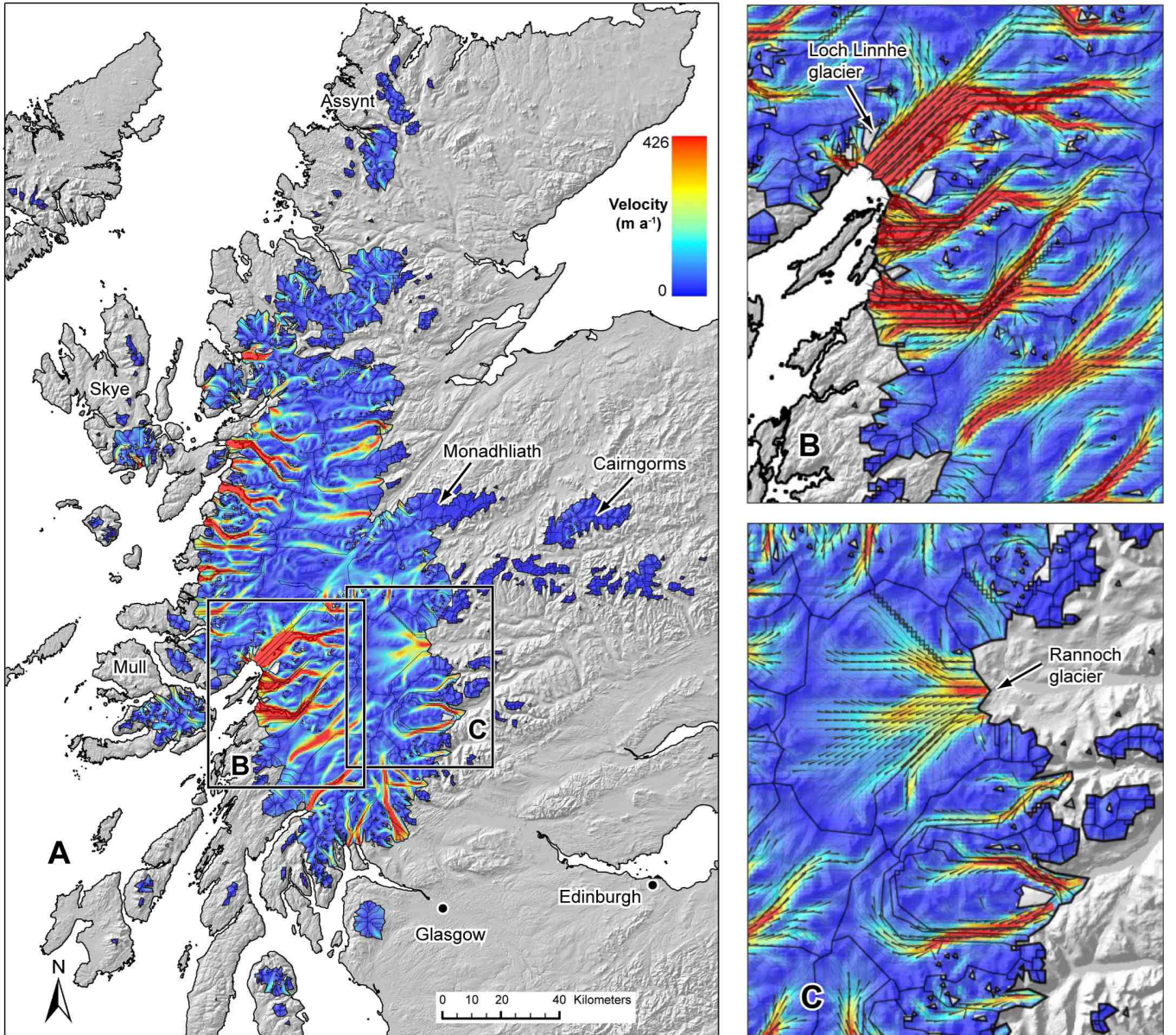


Fig. 3. A: mean velocity distribution in the domain at 2500 model years, boxes locate detail areas B & C. B: detail of Loch Linnhe area glaciers, showing flow vectors and glacier catchments, and C: detail of Loch Rannoch area glaciers, showing flow vectors and glacier catchments. Legend for detail areas same as main figure.

$$S = \frac{(V_s - V_b)}{V_s} - \frac{V_b}{V_s} \quad (4)$$

According to this simple relationship, a value of +1 defines areas flowing entirely by creep, and -1 areas whose total velocity is accounted for by basal motion, assumed to be sliding. Figure 5 shows the spatial variability of dominant flow mechanisms forecast by the relationship, as well as areas where basal velocities are less than 1 ma^{-1} .

The results show concentric zonation of the ice cap in which creep dominates in the interior of the ice cap, and basal sliding becomes most important nearer the margins. This distribution differs significantly from the pattern of mean velocities shown in Figure 3A, in which relatively fast-flowing radial corridors of ice extend considerable distances into glacier accumulation areas from their ablation-zone termini. West-east contrasts are again evident, clearly illustrated by the marked differences between the icefields in Mull, Skye, and Assynt,

and in the Cairngorms and Monadhliath, and in the width of the sliding ‘fringe’ around the main ice cap. Sliding is the dominant mode of flow up to c. 20 km up-glacier from western ice margins and only small areas of immobile ice occur, but in the east, sliding is only dominant in the lower reaches of outlet glaciers, which are separated from one another by extensive areas of immobile ice. This low velocity, non-sliding, ice is mostly associated with ice divides, interflues and plateaux (Figure 5). Although we do not account for it, the possibility exists that sliding may be under-predicted in these eastern areas, however, if the firm is sufficiently warmed by the release of latent heat from percolation and refreezing of seasonal meltwater, as is reported in many Arctic glaciers (e.g. Trabant and Mayo, 1985; Rabus and Echelmeyer, 1998).

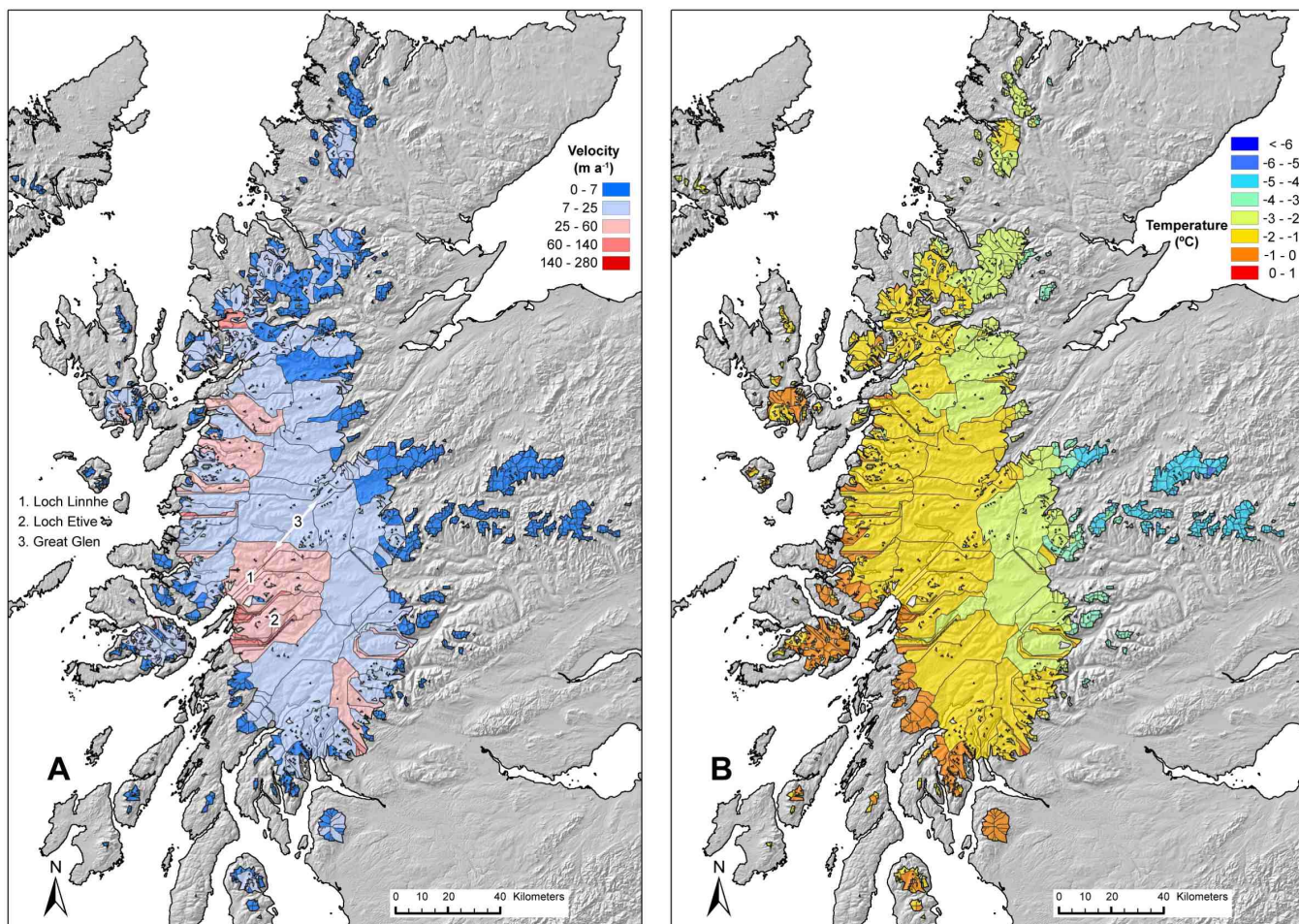


Fig. 4. Model output at 2500 model years showing A: catchment-averaged velocities across the model domain, and B: catchment-averaged mean temperatures. Note the higher values in western areas in both cases.

Basal processes

The relative ability of ice to erode its bed (E) can be approximated from its basal velocity and the overburden pressure resulting from its thickness (H), so that $E = -f |V_b| H$, where f is a constant representing bedrock erodibility (Jamieson and others, 2007). In order to calculate only the spatial pattern of erosion potential exerted by the ice, rather than the amount of basal substrate eroded, we assume a uniform bed rheology and set $f = 1$. Figure 6A shows the areas forecast by this formula to be subjected to greatest potential erosion by the Younger Dryas ice cap. The assumption of a uniform bed hardness probably masks the extent of local variability, but at the domain scale the calculated pattern reflects focussed erosion along major flowlines within the main ice cap. Due to its dependence on ice thickness, erosion potential is considerably less along glacier margins than beneath their trunks. In these mid-sections of glaciers, elongate zones of high erosion potential occur many tens of kilometers up-glacier from glacier termini (Figure 6A). Where ice is thin, such as in many of the outlying icefields, the potential for subglacial erosion is negligible.

Theoretically, where basal ice reaches the pressure melting point, the meltwater produced will either refreeze, permeate into the underlying substrate, or flow along a vector representing the glaciohydraulic gradient. The magnitude of

this gradient is largely governed by the thickness of overlying ice and the topography of the glacier bed. We do not calculate melt here, but use ice thickness and basal topography to identify where meltwater would most likely accumulate and thereafter flow. Figure 6B illustrates the likely routeways for basal meltwater drainage, based on accumulation within subglacial catchments. Given the dependence on ice overburden pressure it is not surprising that the principal drainage paths flow approximately radially from the thick ice cap centre to its thinner margins, along the main valleys that also focus the flow of ice. Although weakly developed arborescent drainage networks may occur in some catchment areas beneath the centre of the ice cap, the majority of subglacial meltwater beneath outlet glaciers is predicted to preferentially follow only one dominant path, giving rise to a distribution of low-order subglacial streams (*sensu* Strahler, 1952) (Figure 6B). These hypothetical subglacial streams largely accord with modern drainage networks, due to the high degree of topographic control exerted by the mountainous relief underlying the majority of the ice cap. Inability to simulate former subglacial and ice-marginal lakes, such as those inferred from geological evidence to have existed during the Younger Dryas in western Scotland (e.g. Ballantyne, 1979; Golledge and Phillips, 2008), remains a limitation of our model and an area where future research may be focussed.

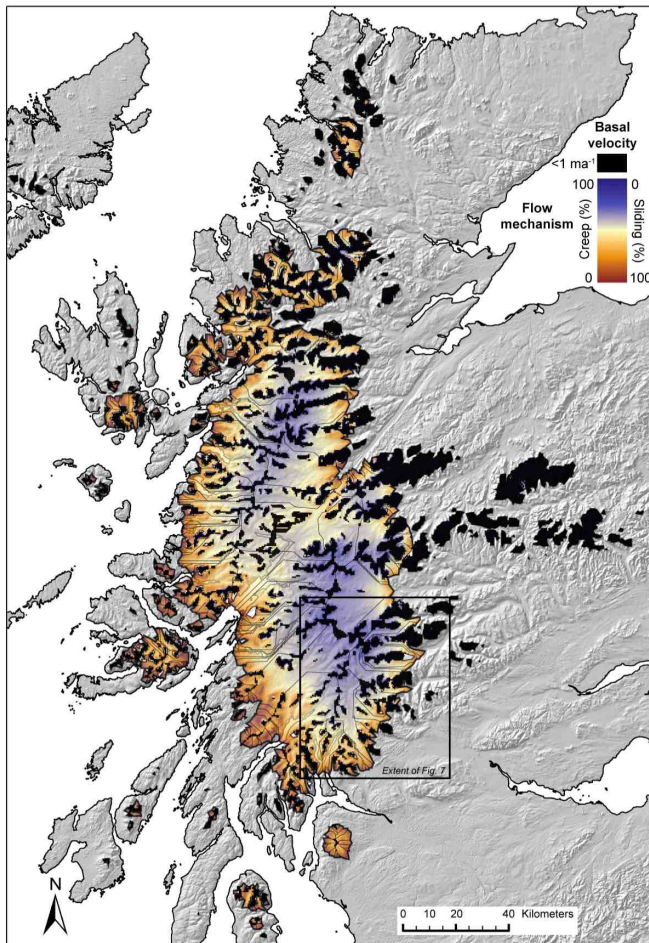


Fig. 5. Calculated proportions of flow by sliding and by creep, (*S*), within the Younger Dryas ice cap and its outlying icefields, at 12.5 ka BP, and areas where ice is effectively immobile, with basal velocities $< 1 \text{ ma}^{-1}$. Note 1) the dominance of internal deformation in central areas of the ice cap, 2) the asymmetry in the width of the marginal fringe of basal sliding, and 3) the far more extensive areas of non-sliding ice in the east.

DISCUSSION AND COMPARISON WITH GEOLOGICAL DATA

The way in which glaciers flow excites considerable debate (Boulton, 1986; Boulton and others, 2001a; Piotrowski and others, 2001, 2002; Kjær and others, 2007), primarily because of the implications associated with the different flow mechanisms. Whereas widespread deformation of unconsolidated basal sediments may play an important role in glacier motion, it is also clear that basal environments are highly complex and vary in both space and time (Piotrowski and others, 2004). Consequently, bed deformation will most likely be accompanied by meltwater-lubricated sliding on rigid beds, as well as flow by the deformation of ice crystals (creep). Whilst our model does not differentiate between basal sliding and deformation of the *bed*, it allows the balance between basal motion and internal deformation of the Scottish Younger Dryas ice cap to be quantified for the first time. Furthermore, it enables the spatial pattern of this variability to be calculated at 500 m resolution. Figure 5 highlights how flow mechanics are partitioned into concentric zones within the ice cap, reflecting down-glacier changes in basal conditions. From this

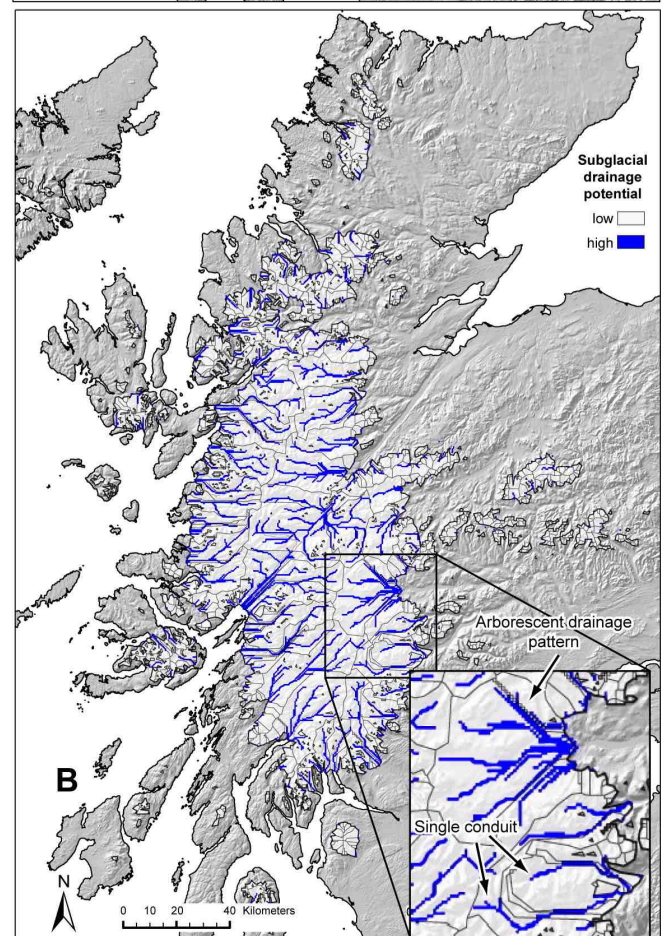
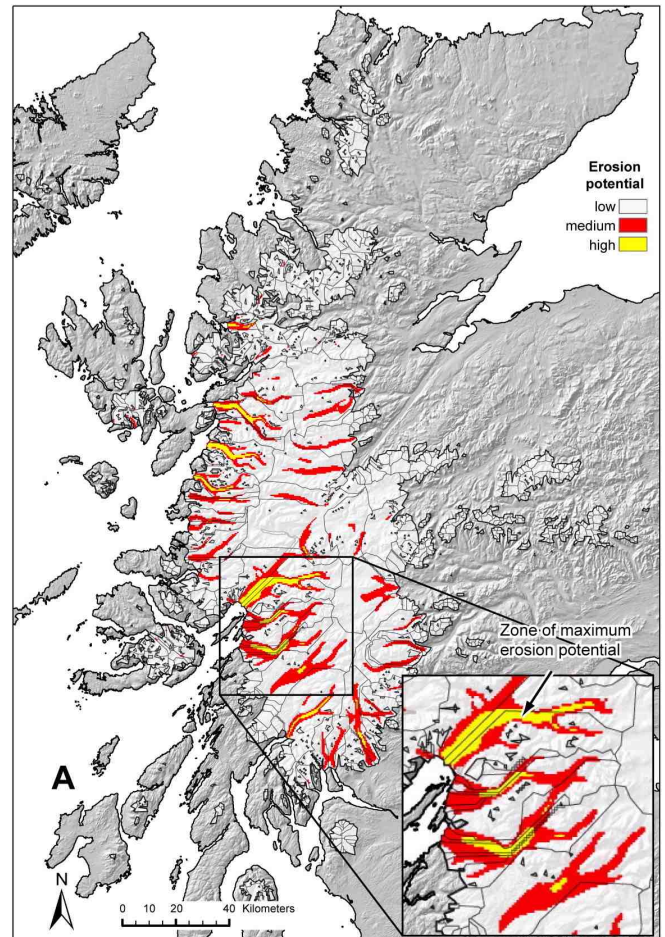


Fig. 6. A: Areas exposed to greatest subglacial erosion potential, based on ice thickness and velocity; inset shows detail. B: likely subglacial drainage pathways calculated from the glaciohydraulic gradient; inset shows detail. Legend for insets same as main figures.

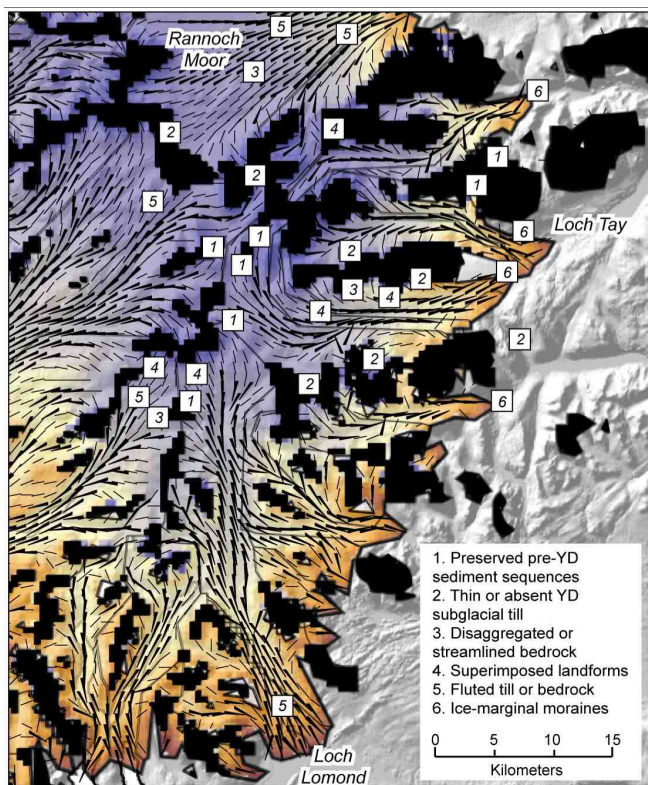


Fig. 7. The southeast sector of the modelled Younger Dryas ice cap, showing locations of geological features described in the text, in relation to areas of immobile, sliding-dominated and creep-dominated zones as described in Figure 5. Glacier flow vectors are also shown.

it may be inferred that deforming beds will only be generated where ice thicknesses and sliding velocities are high, that is, in topographic troughs beneath the ice cap. Accretion of subglacial sediments will occur downglacier of these areas, where ice is thinner but where it is still sliding and able to transport entrained sediment. Glacier recession would have led to spatial changes in the location of these sediment ‘sinks’, thus the thickest deformable sequences probably accumulated at maximal margins with thinner sequences laid down nearer the ice cap core. These model inferences also imply that in some central areas, a deforming substrate may have been either completely absent, or patchy, as a result of the very limited sliding that is forecast to have occurred there. Low velocities in the ice cap core would also have favoured the preservation of pre-existing landscape elements. Transitional areas between non-sliding and sliding ice are likely to have a mixed basal signature. Such areas may host pockets of deformable sediments, partially modified (remoulded) landforms, and unmodified relict landscape components.

Geological mapping in the southeast sector of the ice cap has revealed that thick sequences of sediments *pre-dating* the Younger Dryas are only preserved in topographic hollows near the centre of the ice cap (Golledge, 2007a,b), which, according to the modelled flow patterns, coincide with areas of immobile ice on ice divides between divergent glaciers (Figure 7, ‘1’). Modelled ice divides in this area are also associated with mapped areas *lacking* thick or widespread Younger Dryas subglacial till (Figure 7, ‘2’), presumably due

to the limited erosion and transport capacity of basal ice in such locations. Disaggregated or streamlined bedrock characterised by metre-scale displacement of blocks, (Figure 7, ‘3’) (Golledge, 2006), occurs in locations where the model forecasts the downglacier transition to sliding-dominated ice-flow, perhaps reflecting limited transport of basal substrate previously frozen to the glacier bed. Superimposed bedforms showing cross-cutting lineations (Figure 7, ‘4’), are mapped in areas where the model forecasts either convergent flow or the onset of flow in tributary glaciers feeding a major outlet, whereas more pervasively streamlined (fluted) bedforms (Figure 7, ‘5’) are found where modelled ice-flow is more substantially dominated by basal sliding, rather than creep. Ice-marginal moraines are present throughout the western Highlands, marking successive positions of retreating glaciers. Extensive suites of such moraines thought to represent maximal Younger Dryas glacier limits are shown in Figure 7 (‘6’), adjacent to the sliding termini of discrete outlet glaciers draining the eastern margin of the ice cap.

The pattern of greatest erosion potential (Figure 6A) shows that the greatest work done by outlet glaciers should be concentrated in narrow zones between the core of the ice cap and its margins. Where these zones of high erosion potential coincide with relatively high proportions of flow by basal sliding (Figure 5), the deforming layer is liable to excavation and mobilisation. Fluctuation of glacier margins both through a single glacial episode and over repeated glaciations serves to accentuate these patterns, leading to overdeepened rock basins beneath the mid-sections of outlet glaciers. When the locations of greatest erosion potential forecast by the model (Figure 6A) are compared with the pattern of rock basins in Scotland identified by Sissons (1967), a striking similarity can be seen (Figure 8). That these basins extend beyond the modelled Younger Dryas limits, and probably require repeated glacial cycles to develop, may suggest that the ice configuration achieved at the height of the Younger Dryas perhaps represents a stage that has been reached many times during repeated Pleistocene glaciations.

The discharge of meltwater beneath glaciers influences their rate of flow by changing effective stresses and basal thermal conditions, seen most dramatically in surge-type glaciers (Kamb, 1987; Murray and others, 2000). Understanding the mechanisms of subglacial drainage also greatly assists in the interpretation of the glacial sedimentary sequences (Golledge and Phillips, 2008), and may help to identify areas where glaciofluvial erosion and deposition are most likely to have taken place. Modelled potential drainage patterns for the maximum Younger Dryas ice cap show that subglacial meltwater flow probably followed a small number of low-order paths at the beds of individual outlet glaciers. This ‘conduit’ type system is highly effective at discharging meltwater (Kamb, 1987; Paterson, 1994), and may have been instrumental in maintaining high overburden pressures within the ice cap, and to some extent may have acted as a brake on glacier flow. The considerably increased volume of meltwater generated during deglaciation, however, may have reduced effective stresses sufficiently to promote accelerated flow, and possibly even surge-type behaviour amongst some of the outlets, as inferred from geological evidence for Younger Dryas glaciers in Loch Lomond (Thorp, 1991), and the neighbouring outlet in Menteith (Evans and Wilson, 2006). The influence of

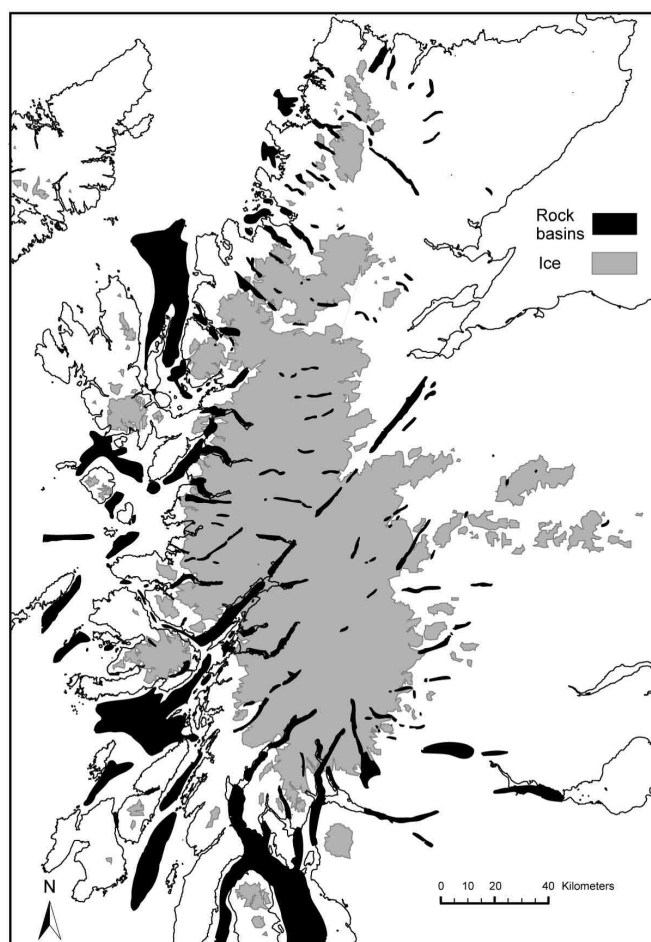


Fig. 8. Rock basins in Scotland, modified from Sissons (1967), and their context in relation to the modelled extent of Younger Dryas ice described here. Note the similarity in general distribution to the pattern of erosion predicted in Figure 6A

a permeable bed on meltwater drainage is not accounted for by the model, however, and so any interpretations of the subglacial hydrologic system can only be regarded as speculative.

Geological investigations north and west of the ice cap centre have identified landforms indicative of thinner, more dynamic glaciers than those inferred in the south and east (e.g. Thorp, 1986; Bennett and Boulton, 1993). These studies have focussed on the relative importance of deforming beds to facilitate flow, rather than internal deformation. By identifying the glaciological contrasts evident between different sectors of the ice cap, the model results presented here go some way towards reconciling these apparently opposing views. The higher velocities, warmer beds, and greater integrated melting ablation occurring in western areas reflect the former presence of high-turnover dynamic corridors within the ice cap that drained the central accumulation areas steeply towards a sea level only slightly higher than present (Shennan and others, 1999). East of the main ice divides, however, topographic slopes are considerably lower, and the palaeoclimate was drier. These less dynamic areas would have experienced less strain heating, raising the effective viscosity of the ice and favouring thicker, more sluggish and probably less erosive glaciers. Whether these thermodynamic contrasts are suf-

ficient to explain the absence of erosional periglacial trimlines in eastern areas, in contrast to their abundance further west, remains an interesting future research avenue (Thorp, 1986; Golledge, 2007a).

CONCLUSIONS

Investigation of the mass balance regime and resultant growth and flow characteristics of numerically simulated Younger Dryas ice masses in Scotland, and their relation to geological evidence, has revealed the following new insights:

1. The modelled ice cap is significantly influenced by spatial contrasts in the climate that gives rise to it, so that it is dynamically asymmetric at its maximum, with western glaciers generally warmer and faster-flowing than their eastern counterparts.
2. Flow in the core of the Younger Dryas ice cap probably occurred primarily through ice deformation, enabling the preservation of older sediments and landforms.
3. Basal sliding dominated the flow of western outlet glaciers, and led to relatively thick Younger Dryas sediment accumulations at their margins. East of the ice cap centre, the modelled ice cover is colder than that in the west, was not sliding at its bed, and had very low erosion potential.
4. The geometry of the modelled ice cap favours focussed basal erosion in the mid-sections of topographic troughs, and gives rise to a pattern of erosion potential that closely matches many of the locations of mapped rock basins in Scotland.
5. The combined influence of ice thickness variability and bed topography produce glaciohydraulic gradients that would have preferentially facilitated basal meltwater drainage along low-order glaciofluvial systems, focussed into central conduits.

ACKNOWLEDGEMENTS

We are grateful to Rhys Cooper for preparation of the digital terrain model, and to Martin Smith and BGS Training for supporting the work. The work benefited significantly from useful discussions with numerous BGS colleagues both in the field and elsewhere. Constructive reviews by Tom Bradwell, Alison Monaghan, Pirjo-Leena Forsström and an anonymous referee significantly improved the paper. NRG publishes with the permission of the Executive Director of BGS (NERC).

References

- Alley, R.B., 2000. The Younger Dryas cold interval as viewed from central Greenland, *Quaternary Science Reviews*, **19**, 213–226.
- Atkinson, T. C., K. R. Briffa and G. R. Coope, 1987. Seasonal temperatures in Britain during the past 22,000 years, reconstructed using beetle remains, *Nature*, **325**, 587–592.
- Ballantyne, C. K., 1979. A sequence of Lateglacial ice-dammed lakes in East Argyll, *Scottish Journal of Geology*, **15**, 153–160.
- Ballantyne, C. K., 1989. The Loch Lomond Readvance on the Isle of Skye, Scotland: glacier reconstruction and palaeo-

- climatic implications., *Journal of Quaternary Science*, **4**, 95–108.
- Ballantyne, C. K., 2002. The Loch Lomond Readvance on the Isle of Mull, Scotland: glacier reconstruction and palaeoclimatic implications., *Journal of Quaternary Science*, **17**, 759–771.
- Benn, D.I., J.J. Lowe and M.J.C. Walker, 1992. Glacier response to climatic change during the Loch Lomond Stadial and early Flandrian: geomorphological and palynological evidence from the Isle of Skye, Scotland., *Journal of Quaternary Science*, **7**, 125–144.
- Benn, D. I., N. R. J. Hulton and R. H. Mottram, 2007a. ‘Calving laws’, ‘sliding laws’ and the stability of tidewater glaciers, *Annals of Glaciology*, **46**, 123–130.
- Benn, D. I., C. R. Warren and R. H. Mottram, 2007b. Calving processes and the dynamics of calving glaciers, *Earth-Science Reviews*, **82**, 143–179.
- Bennett, M.R. and G.S. Boulton, 1993. Deglaciation of the Younger Dryas or Loch Lomond Stadial ice-field in the northern Highlands, Scotland., *Journal of Quaternary Science*, **8**, 133–145.
- Boulton, G. S., 1986. A Paradigm Shift In Glaciology?, *Nature*, **322**, 18.
- Boulton, G. S., K. E. Dobbie and S. Zatsepin, 2001a. Sediment deformation beneath glaciers and its coupling to the subglacial hydraulic system, *Quaternary International*, **86**, 3–28.
- Brooks, S.J. and H.J.B. Birks, 2000. Chironomid-inferred Late-glacial air temperatures at Whitrig Bog, southeast Scotland., *Journal of Quaternary Science*, **15**, 759–764.
- Brown, C., M. Meier and A. Post, 1982. Calving speed of Alaskan tidewater glaciers, with application to Columbia Glacier, *Professional Paper 1258-C*, USGS, 13pp.
- Charbit, S., C. Ritz and G. Ramstein, 2002. Simulations of Northern Hemisphere ice-sheet retreat: sensitivity to physical mechanisms involved during the Last Deglaciation, *Quaternary Science Reviews*, **21**(1-3), 243–265.
- Clapperton, C.M., 1997. Greenland ice cores and North Atlantic sediments: implications for the last glaciation in Scotland., Gordon, J.E., ed., *Reflections on the ice age in Scotland: an update on Quaternary Studies*, Scottish Association of Geography Teachers and Scottish Natural Heritage, 45–58.
- Clark, C.D., D.J.A. Evans, A. Khatwa, T. Bradwell, C.J. Jordan, S.H. Marsh, W.A. Mitchell and M.D. Bateman, 2004. Map and GIS database of glacial landforms and features related to the last British Ice Sheet., *Boreas*, **33**, 359–375.
- Dethloff, K., M. Schwager, J. H. Christensen, S. Kiilsholm, A. Rinke, W. Dorn, F. Jung-Rothenhäusler, H. Fischer, S. Kipfstuhl and H. Miller, 2002. Recent Greenland accumulation estimated from regional climate model simulations and ice core analysis, *Journal of Climate*, **15**, 2821–2832.
- Evans, D. J. A. and S. B. Wilson, 2006. Scottish Landform Example 39: The Lake of Menteith glaciotectionic hill-hole pair, *Scottish Geographical Journal*, **122**, 352–364.
- Glen, J. W., 1955. The creep of polycrystalline ice, *Proceedings of the Royal Society of London, Series A*, **228**, 519–538.
- Golledge, N. R., 2006. The Loch Lomond Stadial glaciation south of Rannoch Moor: new evidence and palaeoglaciological insights, *Scottish Geographical Journal*, **122**, 326–343.
- Golledge, N. R., 2007a. An ice cap landsystem for palaeoglaciological reconstructions: characterizing the Younger Dryas in western Scotland, *Quaternary Science Reviews*, **26**, 213–229.
- Golledge, N. R., 2007b. Sedimentology, stratigraphy, and glacier dynamics, western Scottish Highlands, *Quaternary Research*, **68**, 79–95.
- Golledge, N. R., A. Hubbard and D. E. Sugden, 2008. High-resolution numerical simulation of Younger Dryas glaciation in Scotland, *Quaternary Science Reviews*, doi:10.1016/j.quascirev.2008.01.019.
- Golledge, N. R. and E. R. Phillips, 2008. Sedimentology and architecture of De Geer moraines in the western Scottish Highlands, and implications for grounding-line glacier dynamics, *Sedimentary Geology*, doi:10.1016/j.sedgeo.2008.03.009.
- Hubbard, A., 1999. High-resolution modeling of the advance of the Younger Dryas ice sheet and its climate in Scotland, *Quaternary Research*, **52**, 27–43.
- Hubbard, A., 2000. The verification and significance of three approaches to longitudinal stresses in high-resolution models of glacier flow, *Geografiska Annaler*, **82**, 471–487.
- Hubbard, A., 2006. The validation and sensitivity of a model of the Icelandic ice sheet, *Quaternary Science Reviews*, **25**, 2297–2313.
- Hubbard, A., A. S. Hein, M. R. Kaplan, N. R. J. Hulton and N. Glasser, 2005. A modelling reconstruction of the last glacial maximum ice sheet and its deglaciation in the vicinity of the Northern Patagonian Icefield, South America, *Geografiska Annaler*, **87A**, 375–391.
- Hubbard, A., D. E. Sugden, A. J. Dugmore, H. Norddahl and H. G. Pétursson, 2006. A modelling insight into the Icelandic Last Glacial Maximum ice sheet, *Quaternary Science Reviews*, **25**, 2283–2296.
- Jamieson, S. S. R., N. R. J. Hulton and M. Hagdorn, 2007. Modelling landscape evolution under ice sheets, *Geomorphology*, **92**, 91–108.
- Johnsen, S. J., D. Dahl-Jensen, W. Dansgaard and N. S. Gundestrup, 1995. Greenland palaeotemperatures derived from GRIP bore hole temperature and ice core isotope profiles, *Tellus*, **47**, 624–629.
- Johnsen, S. J., D. Dahl-Jensen, N. S. Gundestrup, J.P. Stefensen, H.B. Clausen, H. Miller, V. Masson-Delmotte, A.E. Sveinbjörnsdóttir and J. White, 2001. Oxygen isotope and palaeotemperature records from six Greenland ice-core stations: Camp Century, Dye-3, GRIP, GISP2, Renland and NorthGRIP, *Journal of Quaternary Science*, **16**, 299–307.
- Kamb, B., 1987. Glacier surge mechanism based on linked cavity configuration of the basal water conduit system, *Journal of Geophysical Research*, **92**(B9), 9083–9100.
- Kjær, K. H., E. Larsen, J. J. M. van der Meer, O. Ingólfsson, J. Krüger, I.O. Benediktsson, C.G. Knudsen and A. Schomacker, 2007. Subglacial decoupling at the sediment/bedrock interface: a new mechanism for rapid flowing ice, *Quaternary Science Reviews*, **25**, 2704–2712.
- Knight, J., 2003. Evaluating controls on ice dynamics in the north-east Atlantic using an event stratigraphy approach, *Quaternary International*, **99-100**, 45–57.
- Kroon, D., W. E. N. Austin, M. R. Chapman and G. M. Ganssen, 1997. Deglacial surface circulation changes in the northeastern Atlantic: Temperature and salinity records off NW Scotland on a century scale, *Paleoceanography*, **12**, 755–763.
- Laumann, T. and N. Reeh, 1993. Sensitivity to climate change

- of the mass balance of glaciers in southern Norway, *Journal of Glaciology*, **39**, 656–663.
- MacAyeal, D. R., 1993. Binge/purge oscillations of the Laurentide Ice-Sheet as a cause of the North-Atlantic Heinrich Events, *Paleoceanography*, **8**, 775–784.
- Mangerud, J., 1991. The last interglacial/glacial cycle in Northern Europe, Shane, L. C. K. and E. J. Cushing, eds., *Quaternary Landscapes*, University of Minnesota Press, 38–75.
- Murray, T., G. W. Stuart, P. J. Miller, J. Woodward, A. M. Smith, P. R. Porter and H. Jiskoot, 2000. Glacier surge propagation by thermal evolution at the bed, *Journal of Geophysical Research*, **105**(B6), 13491–13507.
- Paterson, W.S.B., 1994. *The Physics of Glaciers*, Pergamon, Oxford, 3rd ed.
- Payne, A. and D.E. Sugden, 1990. Topography and ice sheet growth, *Earth Surface Processes and Landforms*, **15**, 625–639.
- Peacock, J. D., D. K. Graham, J. E. Robinson and I. P. Wilkinson, 1977. Evolution and chronology of Lateglacial marine environments at Lochgilphead, Scotland, Gray, J. M. and J. J. Lowe, eds., *Studies in the Scottish Lateglacial Environment*, Pergamon, 89–100.
- Perry, M. and D. Hollis, 2005. The generation of monthly gridded datasets for a range of climatic variables over the United Kingdom, *International Journal of Climatology*, **25**, 1041–1054.
- Piotrowski, J. A., N. K. Larsen and F. W. Junge, 2004. Reflections on soft subglacial beds as a mosaic of deforming and stable spots, *Quaternary Science Reviews*, **23**, 993–1000.
- Piotrowski, J. A., D. M. Mickelson, S. Tulaczyk, D. Krzyszkowski and F. W. Junge, 2001. Were deforming subglacial beds beneath past ice sheets really widespread?, *Quaternary International*, **86**, 139–150.
- Piotrowski, J. A., D. M. Mickelson, S. Tulaczyk, D. Krzyszkowski and F. W. Junge, 2002. Reply to the comments by G.S. Boulton, K.E. Dobbie, S. Zatzepin on: Deforming soft beds under ice sheets: how extensive were they?, *Quaternary International*, **97-8**, 173–177.
- Rabus, B. and K. Echelmeyer, 1998. The mass balance of McCall Glacier, Brooks Range, Alaska, U.S.A.; its regional relevance and implications for climate change in the Arctic, *Journal of Glaciology*, **44**, 333–351.
- Shennan, I., M. J. Tooley, F. Green, J. Innes, K. Kennington, J. Lloyd and M. Rutherford, 1999. Sea level, climate change and coastal evolution in Morar, northwest Scotland, *Geologie en Mijnbouw*, **77**, 247–262.
- Siegert, M.J. and J.A. Dowdeswell, 2004. Numerical reconstructions of the Eurasian Ice Sheet and climate during the Late Weichselian, *Quaternary Science Reviews*, **23**, 1273–1283.
- Sissons, J.B., 1979. The Loch Lomond Stadial in the British Isles, *Nature*, **280**, 199–203.
- Sissons, J. B., 1967. *The Evolution of Scotland's Scenery*, no. 259pp, Oliver & Boyd, Edinburgh.
- Strahler, A. N., 1952. Dynamic basis of geomorphology, *Geological Society of America Bulletin*, **63**, 923 – 938.
- Sutherland, D. G., 1984. The Quaternary deposits and landforms of Scotland and the neighboring shelves - a review, *Quaternary Science Reviews*, **3**, 157–254.
- Thorp, P.W., 1986. A mountain icefield of Loch Lomond Stadial age, western Grampians, Scotland, *Boreas*, **15**, 83–97.
- Thorp, P.W., 1991. Surface profiles and basal shear stresses of outlet glaciers from a Late-glacial mountain ice field in western Scotland, *Journal of Glaciology*, **37**, 77–88.
- Trabant, D. and L. Mayo, 1985. Estimation and effects of internal accumulation on five glaciers in Alaska, *Annals of Glaciology*, **6**, 113–117.
- van der Veen, C. J., 1999. *Fundamentals of glacier dynamics*, no. 462pp, Balkema, Rotterdam.
- Zweck, C. and P. Huybrechts, 2003. Modeling the marine extent of Northern Hemisphere ice sheets during the last glacial cycle, *Annals of Glaciology*, **37**, 173–180.